International Society for Rock Mechanics and Rock Engineering
Norwegian Group for Rock Mechanics

ISRM International Symposium
Eurock 2025 – Expanding the Underground Space
Trondheim, Norway, 16-20 June
ISBN 978-82-8208-079-8

Assimilation of drilling data for predicting ground deformation during tunnel construction

Y. Aono, S. Yamamoto, H. Sakurai & H. Tada
Shimiz Corporation, Tokyo, Japan
y.aono@shimz.co.jp

T. Okuno
Fukada Geological Institute, Tokyo, japan

M. Kikumoto
Yokohama National University, Kanagawa, Japan

Abstract

The support design and excavation planning of underground structures, including mountain tunnels and underground power plants, are often updated based on the results of ground deformation measurements and tunnel face observations. As these design changes are sometimes examined through numerical analysis, it is necessary to account for various uncertainties, such as initial and boundary conditions, geological structures, and mechanical properties of rocks. This study investigates the application of ensemble-based data assimilation (EBDA) to achieve highly reliable predictions of ground deformation during construction. An excavation analysis method incorporating EBDA was developed and applied to ground tunneling scenarios, assuming an elasto-plastic model. The effect of assimilating the displacements of ground and the uniaxial compressive strength q_u were confirmed in this analysis. It is assumed that q_u is converted from the drilling energy. q_u is related to cohesion c and friction angle φ. By assimilating q_u, c converged to the correct value, however since the effect of φ on q_u is small compared to c, significant variation was observed in the φ. In addition, since the displacement of the ground in the already excavated area is not dominant in updating the deformation coefficient E of the ground ahead of the face, the variance of E was not improved. Therefore, resulting in limited improvements in estimating the Mohr-Coulomb failure criterion line and the predicting ground displacement.

Keywords

Ensemble-based data assimilation, Underground structures, Numerical analysis, Drilling data

ISRM

NBG

1 Introduction

During the construction of underground structures, such as mountain tunnels and underground power plants, daily tunnel face observations and ground displacement measurements are conducted to evaluate the behavior of the surrounding rock mass. These observations and measurements support adjustments to initial support designs and construction methods to align with actual ground conditions, often referencing prior construction results. Numerical analyses are occasionally employed to address unexpected phenomena, such as excessive ground deformation and tunnel face instability. However, these analyses face challenges due to several uncertainties in geological structures, rock properties, and initial and boundary conditions, which considerably complicate numerical modelling. Against this problem, several approaches have studied for predicting ground properties and displacements using observed data collected during the construction. For instance, Shuku et al. (2011) employed data assimilation (DA) to predict embankment behavior, highlighting its ability to provide probabilistic evaluations and enhance prediction reliability.

Muhammad et al. (2021) applied the ensemble Kalman filter (EnKF) (Evensen, 1994) to estimate the physical parameter of a slope assuming an elastic-perfectly plastic model and a strain-hardening model to evaluate the stability of the slope. Yu et al. (2021) utilized a hierarchical Bayesian model to estimate the average stress of the rock mass. They showed that the uncertainty of the average stress in the target area can be reduced by using information on the rock mass stress measured near the target area. In addition, data assimilation techniques have also been used to predict the amount of spring water for mountain tunnels under construction. Koyama et al. (2012) integrated the EnKF algorithm into the system for water information of ground (SWING) method to automate the optimization process of parameters for groundwater analysis and predicted the spring water flow.

Given the heterogeneous nature of the ground and uncertainties in mechanical properties, reliably quantify predictions of ground and support behavior in tunnel construction is essential. This requires integrating observation and analysis data, as demonstrated in above previous studies. The authors have previously investigated a method for predicting deformation behavior of ground by combining the finite volume method (FVM) and data assimilation techniques. We have previously conducted numerical experiments simulating tunnel construction into ground assuming elastic and elasto-plastic models, as well as numerical experiments simulating triaxial compression tests on rock specimen assuming an elastoplastic model (e.g., Aono et al, 2021, 2022, 2023). In these numerical experiments, displacement data of the ground at already excavated areas and rock specimen was used for assimilation. It was confirmed that prediction performance of the deformation behavior of the ground and rock specimen after assimilation. As a result, it was found that assimilating only displacement data at already excavated areas was insufficient for early prediction of the behavior of the unexcavated ground ahead of the tunnel face.

As a next phase, the authors focused on drilling logging, a forward exploration method, to improve the performance of prediction of ground deformation behavior at early construction stage. A method has been reported to convert the drilling energy obtained by drilling logging into the unconfined compressive strength, q_u (e.g., Yamashita et al., 2015). The authors conducted numerical experiments simulating loading test using a single element (this corresponds to the zone in FVM) and confirmed that assimilation of q_u improves the prediction performance of the deformation behavior of the analytical model (Aono et al, 2024). In this paper, the effectiveness of assimilating ground displacement and q_u in estimating the physical properties and predicting deformation behavior of the ground was demonstrated through numerical experiments simulating tunnel construction assuming heterogeneous ground including geological boundaries.

2 DA for excavation analysis

Several DA methods employ commonly used sequential and ensemble-based DA techniques including EnKF and particle filter (PF). EnKF-base methods requires inverse matrix calculations which are computationally more expensive than PF-base methods, however it has the advantage of being less prone to degeneracy. In contrast, degeneracy is less likely to occur with EnKF-based methods, as these methods update the state variables of each ensemble member to align with the observation. Among EnKF-type methods, we adopted the error subspace transform Kalman filter (ESTKF) (Nerger et al., 2012), which offers a lower computational cost and generally provides superior assimilation results compared to EnKF. The ESTKF is derived from the ensemble transform Kalman filter (ETKF) (Bishop et al., 2001), which is an EnKF-type method.

Below is an overview of the ESTKF and its application to tunnel excavation analysis with DA. In the ESTKF, the state-space model is formulated as follows:

$$\mathbf{x}_n^{\mathrm{FVM}} = \mathrm{f}(\mathbf{x}_{n-1}, \mathbf{v}_n) \tag{1}$$
$$\mathbf{y}_n = \mathbf{H}\mathbf{x}_n^{\mathrm{FVM}} + \boldsymbol{\omega}_n \quad , \boldsymbol{\omega}_n \sim N(\mathbf{0}, \mathbf{R}) \tag{2}$$

Here, $\mathbf{x}$ is a state vector consisting nodal displacements, element stresses, ground properties and q_{u}; $\mathbf{v}$ represents the system noise; the subscript FVM refers to the results from the finite volume method (FVM) analysis before DA (prior distribution). The subscript n denotes the construction step. $\mathbf{f}$ is an operator that expresses the time evolution of the variables from construction step n–1 to n, corresponding to the excavation analysis performed by FVM using the commercial software FLAC3D. $\mathbf{y}$ is a vector consisting of the displacements caused by excavation at the observation point (hereafter referred to as the observation vector) and q_{u}, with $\mathbf{H}$ being the linear observation operator. $\boldsymbol{\omega}$ represents the observed noise, which follows a normal distribution with mean 0 and covariance matrix $\mathbf{R}$. The state variables are updated based on the observed data using the ESTKF, which is expressed as:

$$\mathbf{X}_n^{\mathrm{DA}} = \overline{\mathbf{X}}_n^{\mathrm{FVM}} + \mathbf{X}_n^{\mathrm{FVM}}\mathbf{T}(\mathbf{w} + \mathbf{W}) \tag{3}$$
$$\mathbf{w} = \mathbf{A}(\mathbf{H}\mathbf{X}_n^{\mathrm{FVM}}\mathbf{T})^{\mathrm{T}}\mathbf{R}^{-1}(\mathbf{Y}_n - \mathbf{H}\mathbf{X}_n^{\mathrm{FVM}}) \tag{4}$$
$$\mathbf{W} = \sqrt{(N-1)}\mathbf{C}\mathbf{T}^{\mathrm{T}} \tag{5}$$
$$\mathbf{A}^{-1} = (N-1)\mathbf{I} + (\mathbf{H}\mathbf{X}_n^{\mathrm{FVM}}\mathbf{T})^{\mathrm{T}}\mathbf{R}^{-1}\mathbf{H}\mathbf{X}_n^{\mathrm{FVM}}\mathbf{T} \tag{6}$$
$$\mathbf{C}\mathbf{C}^{\mathrm{T}} = \mathbf{A} \tag{7}$$
$$T_{\mathrm{ij}} = \begin{cases} 1 - \dfrac{1}{\sqrt{N} + N} & \text{for i} = \text{j, i} < N \\ \dfrac{1}{\sqrt{N} + N} & \text{for i} \neq \text{j, i} < N \\ -\sqrt{N} & \text{for i} = N \end{cases} \tag{8}$$

$$\mathbf{X}_n^{\mathrm{DA}} = (\mathbf{x}_{n,1}^{\mathrm{DA}}, \dots, \mathbf{x}_{n,N}^{\mathrm{DA}}) \tag{9}$$
$$\overline{\mathbf{X}}_n^{\mathrm{FVM}} = (\overline{\mathbf{x}}_n^{\mathrm{FVM}}, \dots, \overline{\mathbf{x}}_n^{\mathrm{FVM}}) \tag{10}$$
$$\mathbf{X}_n^{\mathrm{FVM}} = (\mathbf{x}_{n,1}^{\mathrm{FVM}}, \dots, \mathbf{x}_{n,N}^{\mathrm{FVM}}) \tag{11}$$
$$\mathbf{Y}_n = (\mathbf{y}_n, \dots, \mathbf{y}_n) \tag{12}$$

$\mathbf{x}_n^{\mathrm{FVM}}$ is updated using the projection matrix $\mathbf{T}$, weight vector $\mathbf{w}$ and matrix $\mathbf{W}$. $\mathbf{T}$ is calculated from the number of samples in the ensemble N. $\mathbf{w}$ and $\mathbf{W}$ are calculated by Eq. (4) and (5), respectively. $\mathbf{A}$ and $\mathbf{C}$ are transformation matrices. $\overline{\mathbf{x}}_n^{\mathrm{FVM}}$ represents the ensemble mean of the state vectors. The superscript DA denotes the posterior distribution after DA. In sequential DA of ESTKF, the simulation proceeds through repeated predictions (using Eq. (1)), followed by updates (via Eq. (3)). In a previous study, to ensure the physical relationship between the ground properties and nodal displacements, the authors employed a method where they returned to the stage before excavation. They then added the updated ground parameters from DA to the analytical model, and subsequently re-performed the excavation analysis (Aono et al. 2022). The numerical experiments mentioned at chapter 3 were conducted using this proposed method. Therefore, in this paper, the procedures of the forward analysis and DA are considered as one DA cycle.

Fig. 1 provides an overview of the ground displacement prediction using this method.

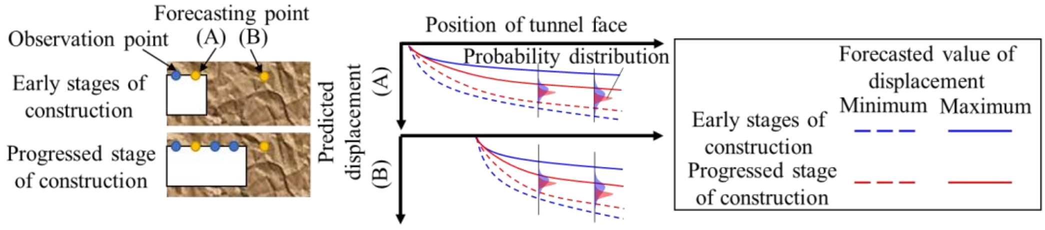

(a) schematics of the longitudinal section along the tunnel axis

(b) Relationship between predicted displacement at forecasting point and position of tunnel face

Fig. 1 Overview of excavation analysis applying DA.

Fig.1 (a) depict schematics of the longitudinal section along the tunnel axis, with the blue and yellow circles representing the observation and prediction points for displacement, respectively. The upper longitudinal section illustrates the early excavation stage, with a limited number of observation points, while the lower section shows the advanced stage, with a greater number of observation points. Fig.1 (b) plots the predicted cumulative displacement for the first two excavation steps. The horizontal axis represents the tunnel face position, with the vertical axis indicating the predicted displacement. The blue and red lines denote predictions at the early and advanced stages of excavation, with the solid and dashed lines indicating the smallest and largest predicted values, respectively. This method quantitatively demonstrates prediction reliability as a probability distribution, with prediction accuracy improving as the number of observation points increases.

3 Outline of numerical experiments

This section provides an overview of the numerical experiment simulating the tunnel construction. In this experiment, the results calculated using an analytical model with correct conditions (referred to as the "correct model") were used as the observed data. These measurement data were then sequentially assimilated into the predicted results from a predictive model (ensemble member), which had different conditions from the correct model. The experiment yielded the distribution of ensemble members relative to the true value, allowing for the verification of the effectiveness of DA for this problem. This study focused on the following key questions points: (i) How are the physical properties of the ground in the prediction model updated through DA? and (ii) How do the predicted results for ground displacement change in the prediction model?

The analysis mesh and observed points of the ground displacement are shown in Fig. 2. The displacement observation point was set at tunnel distance (TD) 2m.

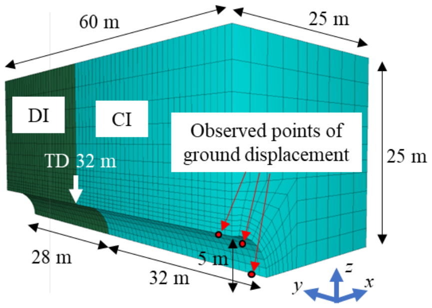

Fig. 2 Numerical model for excavation analysis.

The constitutive model of the rock mass was an elastic-perfectly plastic model, using the Mohr-Coulomb failure criterion. The analysis mesh for the ground was composed of two types of geological features. Table 1 lists the physical properties of the correct model and those used to generate the initial ensemble member.

Table 1. Physical properties of rock mass corresponding to CI and DI patterns.

	E_{CI} (MPa)	E_{DI} (MPa)	c_{CI} (MPa)	c_{DI} (MPa)	φ_{CI} (°)	φ_{DI} (°)	$q_{u,CI}$ (MPa)	$q_{u,DI}$ (MPa)
Correct value	2000	500	2.0	0.4	45	35	9.66	1.54
Range for obtaining the initial distribution of the ensemble	0 - 5000		0 - 4.0		0 - 50		0 - 22.0	

The physical properties of each geological feature were based on the classification of The Japan Highway Public Corporation (1986). The subscripts CI and DI in Table 1 correspond to this classification. However, steel supports, shotcrete, RB were not modelled in this numerical experiment. The geological boundary was set at TD 32m. The position, strike, and dip of the geological boundary surface were identical for both the correct model and the ensemble member, assuming that geological structure information was obtained through prior surveys. DA was performed every 2 m of excavation, from TD 4 m to TD 12 m, resulting in a total of five DA cycles.

In Table 1, E represents the deformation modulus of ground. The physical properties of the correct model were set based on the reference from West Nippon Expressway Company Limited (2018). To understand the changes in the state vector distribution, the range of physical properties for the initial ensemble member was set to values lower than those of the ground corresponding to support pattern B. These properties of the initial ensemble members were set using uniform random numbers from the ranges listed in Table 1. For both the correct model and the predictive model, the Poisson's ratio ν of the ground corresponding to support patterns CI and DI was set to 0.30 and 0.35, respectively. An isotropic pressure equivalent to 300 m of overburden was applied to all elements in the initial stress analysis.

In this paper, we present the results of two numerical experiments in which the information used for assimilation was varied. In Case 1, only the history of displacement increments $\boldsymbol{d}$ in the x, y, and z components of the observation point at TD 2 m were assimilated every 2 m of excavation. In Case 2, $\boldsymbol{d}$ and q_u were assimilated. It was assumed that qu was converted from drilling data obtained through rock bolt (RB) construction and non-core drilling logging ahead of the tunnel face. The effectiveness of assimilating q_u was validated by the results of these numerical experiments.

The numerical experimental procedure is as follows:

At first, an excavation analysis was performed under the correct conditions to generate the simulated observed values (observation vectors) for ground displacement and q_u.

Afterwards, the state vector was created by conducting excavation analysis up to excavation step n, using 50 ensemble members under various conditions. The initial distribution of the ensemble properties was obtained from the ranges shown in Tables 1 using uniform random numbers. Fig. 3 illustrates the displacement observation points and the locations of the elements used for calculating q_u.

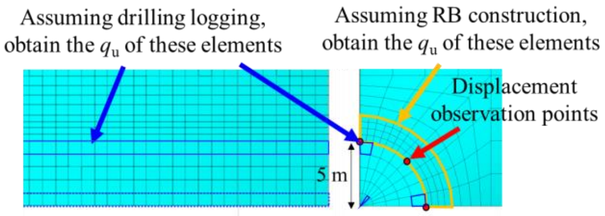

Fig. 3 Displacement observation points and element positions used for calculating q_u.

q_u was calculated using Eq. (13), assuming RB installation and drilling logging:

$$q_u = \frac{2c\cos\varphi}{1-\sin\varphi} \tag{13}$$

Subsequently, the state vectors **x** and **y**, generated by excavation analysis using both the correct condition and ensemble members, were assimilated. The parameters listed in Table 1 were then updated. If any updated parameters were not realistic (for example, negative values or φ > 90°), they were regenerated within the ranges presented in Table 1. DA generally reduces parameter variation; if the variance in the distribution after updating was exceedingly small, the physical properties did not change significantly during the subsequent DA. Therefore, a noise of –10 to 10% of the ensemble mean was added to each parameter after updating. Excavation analysis was then performed up to the next excavation step n+1. The observation errors for the displacement and q_u were set to 1.0 mm and 1.6 MPa, respectively. The observation noise was not considered in the numerical experiment.

4 Results and discussions

4.1 Estimation of ground properties

Fig. 4 shows the ground properties before and after each DA cycles for Cases 1 and 2. In Fig. 4, the black horizontal lines represent the correct values, while blue circles indicate the distribution of the ground properties used in the excavation analysis. Orange triangles denote the updated distribution after DA. Focusing on E_{CI} and E_{DI}, the figure shows that E_{CI} converged to the correct value in both cases, whereas the distribution of E_{DI} exhibited slight changes. These results suggest that displacement observation of the ground from the already excavated area and q_u, assumed to be derived from the drilling data, have minimal influence on the estimation of the ground's Young's modulus (E) approximately 30 m ahead of the face.

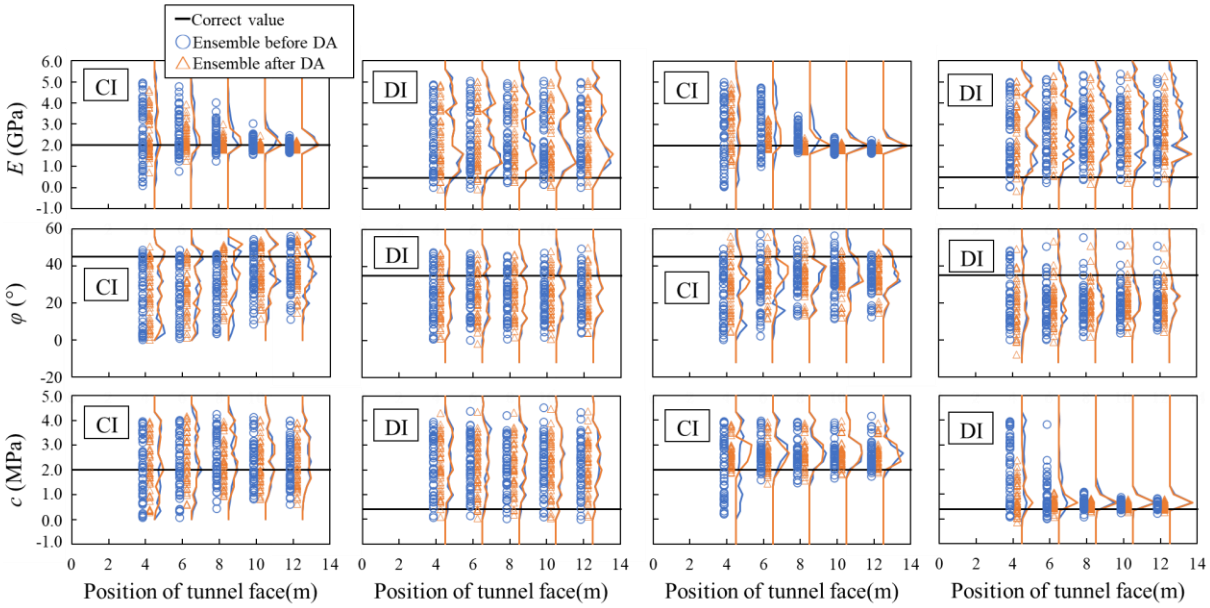

(a) Case1 (b) Case2

Fig. 4 Distribution of physical properties before and after performing DA.

Regarding the friction angles (φ_{CI} and φ_{DI}), Fig. 4 indicates smaller variation in Case 2 compared to Case 1, with the values converging to values below the correct value. As shown in Fig. 4(a), the distributions of c_{CI} and c_{DI} remain unchanged in Case 1, where only $\boldsymbol{d}$ was assimilated. In contrast, in Case 2, the variances of c_{CI} and c_{DI} decreased due to the assimilation of q_u (as seen in Fig. 4(b)), converging to values higher than the correct value. Examining the distribution of the initial ensemble, φ was smaller and c was larger than the correct value in most ensembles. This suggests that the post-DA distributions of φ and c in Case 2 were influenced by the characteristics of the initial ensemble distribution.

Fig. 5 shows the relationship between q_u, φ and c when φ and c change.

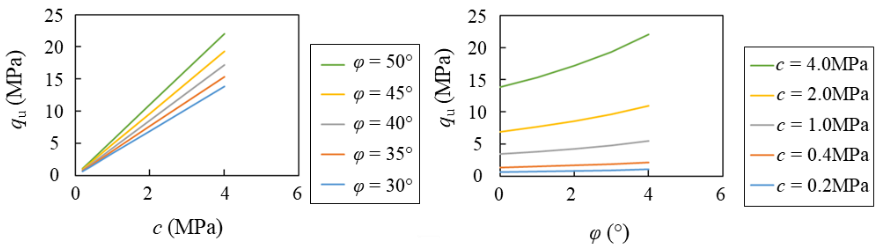

Fig. 5 Relationship between q_u, c, and φ.

According to Fig.5, changing c increases q_u more than changing φ. Since c has a greater effect on q_u than on φ, it is believed that the assimilation of q_u significantly changes the distribution of c.

Furthermore, focusing on the distribution of c_{CI} in Fig. 4(b), its variance is larger than that of c_{DI}. The results from Case 1 show that $\boldsymbol{d}$ has limited significance in updating the physical properties of the ground ahead of the tunnel face; however, it plays a more critical role in already excavated areas. Therefore, by incorporating substantial information from the excavated areas, such as $\boldsymbol{d}$ and q_u, in the assimilation process, the variance of c may increase.

4.2 Prediction of deformation behavior of ground

Fig. 6 illustrates the relationship between the displacement in the z-axis direction at the crown of TD 32 m and the position of the tunnel face when the tunnel was constructed up to TD 60 m. The black, blue, and orange lines represent the absolute ground displacements obtained from the excavation analysis of the correct model, the initial ensemble, and the ensemble after five DA cycles, respectively. The line on the right side of the graph shows the frequency distribution of the displacement when the tunnel face reached TD 60 m.

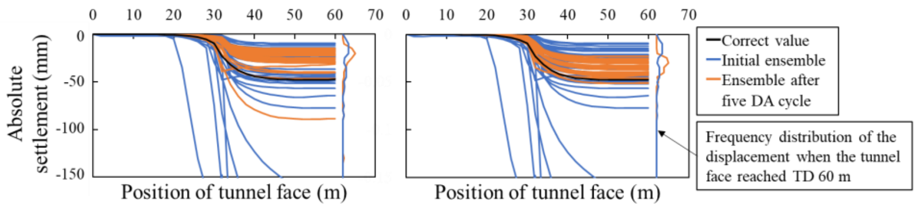

Fig. 6 Predicted crown settlement at TD60m before and after performing five DA cycles.

By repeatedly performing DA, the variance in the predicted results of the ground deformation behavior was reduced in both cases. The differences between the most frequent values of the frequency distribution of the predicted displacement results and the correct values for Cases 1 and 2 were approximately 30 mm and 20 mm, respectively. In both cases, the distribution of E_{DI} remained almost unchanged after DA. As E_{DI} was distributed to values larger than the correct value, the ground displacement was consequently underestimated.

Fig. 7 shows the Mohr stress circle for the correct model and the Mohr-Coulomb failure criterion. The orange lines in Fig. 7 represent the failure criterion of the ensembles after five DA cycles.

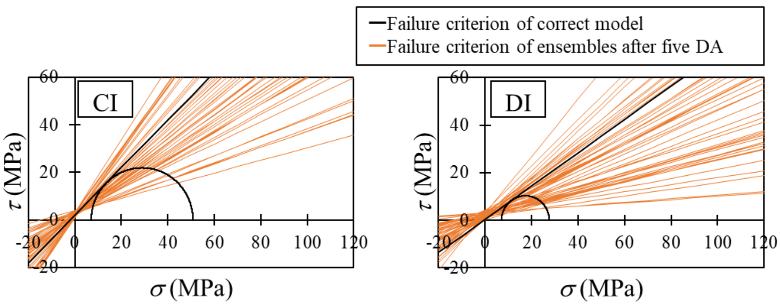

(a) Case1

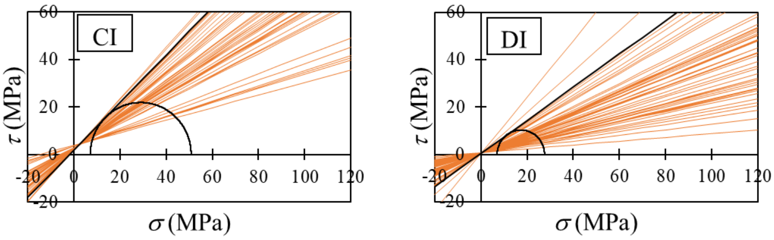

(b) Case2

Fig. 7 Mohr's stress circle of the correct model and Mohr-Coulomb failure criterion.

An isotropic pressure equivalent to 300 m of overburden was applied to all elements, and a Mohr's circle was drawn based on the overburden pressure. As shown in Figs. 4 and 5, as φ could not be estimated in either case, the failure envelopes of the ensemble after five DA cycles differed from the correct envelope. If the failure envelope cannot be estimated accurately, it becomes impossible to precisely predict the plastic deformation of the ground as the stress state changes during tunnel construction. Therefore, it is crucial to estimate φ along with c. Furthermore, when only elastic deformation occurs in the ground, estimating E is essential for accurately predicting the deformation behavior.

To improve the accuracy of estimating E and φ, we are considering creating a regression equation based on the relationship between q_u and the physical properties from West Nippon Expressway Company Limited (2018). This will be followed by assimilating the physical properties converted from q_u using this regression equation. In the future, we plan to assimilate E and φ converted from q_u to examine whether this approach can enhance the accuracy of estimating the physical properties of the ground and predicting its deformation behavior.

5 Conclusion

This paper presents an excavation analysis employing EnKF-base data assimilation for the construction of underground structures, such as mountain tunnels and underground power plants. The focus was on the effect of assimilating the uniaxial compressive strength of the ground (q_u), derived from drilling energy, through numerical experiments simulating tunnel construction in the ground with geological boundaries.

The results demonstrated that the assimilation of q_u significantly reduced the variability in the cohesion c. However, even when q_u was assimilated, the variations in the deformation modulus E and friction angle φ remained larger than those in c. This is likely because, based on the relationship between q_u, φ, and c, variations in c have a greater effect on q_u than variations in φ. Furthermore, the study demonstrated that assimilating only displacement observation from the excavated ground and q_u was insufficient to accurately estimate E in the ground ahead of the tunnel face.

Future work will involve numerical experiments to assimilate E and φ derived from q_u. This will aim to improve the estimation accuracy of these properties ahead of the tunnel face and enhance prediction accuracy of ground deformation behavior during tunnel construction.

References

Aono, Y. and Okuno, T.: Data Assimilation for Prediction of Surrounding Rock Mass Behavior during Underground Structure Construction Phases, 15th ISRM Congress 2023 & 72nd Geomechanics Colloquium, pp.2013-2018, 2023.

Aono, Y., Sakurai, H. and Yamamoto, S.: Prediction for Behavior of Underground Structures during Construction Phase Using Data Assimilation, The 15th World Congress on Computational Mechanics & the 8th Asian Pacific Congress on Computational, p.1766, 2022.

Aono, Y., Sakurai, H. and Yamamoto, S.: Prediction Method for Behavior of Underground Structures during Construction Phase Using Ensemble-based Data Assimilation, Transactions of the Computational Engineering and Science, Vol.26, E-03-02, 2021.

Aono, Y. Yamamoto, S. Kamada, H. and Sakurai, H.: Utilization of Drilling Data in Data Assimilation of Laboratory Rock Test for Behavior Prediction of Underground Structures During Construction Phase, Proceedings of 50th Symposium on Rock Mechanics, pp.175-180, 2024.

Bishop, C. H., Etherton, B. J., Majumdar, S. J.: Adaptive sampling with the ensemble transform Kalman filter. Part I：theoretical aspects, Monthly Weather Review, pp.420-436, 2001.

Evensen, G.: Sequential data assimilation with a nonlinear quasi-geostrophic model using Monte Carlo methods to forecast error statistics, Journal of Geophysical Research, 99(5), pp.10143-10162, 1994.

Itasca Consulting Group, Inc.: Itasca Software Documentation, https://docs.itascacg.com/itasca900/contents.html, (accessed 2024-12-15).

Japan Highway Public Corp: Third-Volume Tunnel Construction Major Designing Points, 1986.

Koyama, T. Kogiso, J. Takahashi, K. Yasuda, T. and Ohnishi, Y.: Development of swing method with sequential data assimilation (SDA-SWING) and its application to groundwater problems in real tunnel construction, Tunnelling and Underground Space Technology, Vol.28, pp.229-237, 2012.

Muhammad, M., Philip, J. V. and Femke, C. V.: On the use of different constitutive models in data assimilation for slope stability, Computers and Geotechnics, vol.138, 104332, 2021.

Nerger, L., Janjić, T., Schröter, J., and Hiller, W.: A unification of ensemble square root Kalman filters: Monthly Weather Review, pp.2335-2345, 2012.

Shuku, T., Murakami, A., Fujisawa, K. and Nishimura, S.: Data Assimilation in Geotechnical Engineering, Geotechnical engineering magazine, Japanese Geotech-nical Society, Vol.59, pp.8-11, 2011.

Yamashita, M. Takemura, I. Sugimoto, T. Yoshinaga, K. and Maeda, K.: Development and application of a prediction and analysis system for tunnel deformation "PAS-Def", Nishimatsu Corporation Technical report, Vol.38, 2015.

Yu, F., Arnaud, G. Ke. M. and Jiawei, L.: Improving local mean stress estimation using Bayesian hierarchical modelling, International Journal of Rock Mechanics & Mining Sciences, Vol.148, 104924, 2021.

West Nippon Expressway Company Limited: Numerical Analysis Manual for Tunnels, p.2-13, 2018.